Monthly Notices of the ROYAL ASTRONOMICAL SOCIETY LETTERS

Mon. Not. R. Astron. Soc. **409,** L1–L6 (2010) doi:10.1111/j.1745-3933.2010.00916.x

Measures of star formation rates from infrared (*Herschel*) and UV (*GALEX*) emissions of galaxies in the HerMES fields

V. Buat,[1⋆] E. Giovannoli,[1] D. Burgarella,[1] B. Altieri,[2] A. Amblard,[3] V. Arumugam,[4] H. Aussel,[5] T. Babbedge,[6] A. Blain,[7] J. Bock,[7,8] A. Boselli,[1] N. Castro-Rodríguez,[9,10] A. Cava,[9,10] P. Chanial,[6] D. L. Clements,[6] A. Conley,[11] L. Conversi,[2] A. Cooray,[3,7] C. D. Dowell,[7,8] E. Dwek,[12] S. Eales,[13] D. Elbaz,[5] M. Fox,[6] A. Franceschini,[14] W. Gear,[13] J. Glenn,[11] M. Griffin,[13] M. Halpern,[15] E. Hatziminaoglou,[16] S. Heinis,[1] E. Ibar,[17] K. Isaak,[13] R. J. Ivison,[4,17] G. Lagache,[18] L. Levenson,[7,8] C. J. Lonsdale,[19] N. Lu,[7,20] S. Madden,[5] B. Maffei,[21] G. Magdis,[5] G. Mainetti,[14] L. Marchetti,[14] G. E. Morrison,[22,23] H. T. Nguyen,[7,8] B. O'Halloran,[6] S. J. Oliver,[24] A. Omont,[25] F. N. Owen,[19] M. J. Page,[26] M. Pannella,[19] P. Panuzzo,[5] A. Papageorgiou,[13] C. P. Pearson,[27,28] I. Pérez-Fournon,[9,10] M. Pohlen,[13] D. Rigopoulou,[27,29] D. Rizzo,[6] I. G. Roseboom,[24] M. Rowan-Robinson,[6] M. Sánchez Portal,[2] B. Schulz,[7,20] N. Seymour,[26] D. L. Shupe,[7,20] A. J. Smith,[24] J. A. Stevens,[30] V. Strazzullo,[19] M. Symeonidis,[26] M. Trichas,[6] K. E. Tugwell,[26] M. Vaccari,[14] E. Valiante,[15] I. Valtchanov,[2] L. Vigroux,[25] L. Wang,[24] R. Ward,[24] G. Wright,[17] C. K. Xu[7,20] and M. Zemcov[7,8]

[1]*Laboratoire d'Astrophysique de Marseille, OAMP, Université Aix-marseille, CNRS, 38 rue Frédéric Joliot-Curie, 13388 Marseille Cedex 13, France*
[2]*Herschel Science Centre, European Space Astronomy Centre, Villanueva de la Cañada, 28691 Madrid, Spain*
[3]*Department of Physics & Astronomy, University of California, Irvine, CA 92697, USA*
[4]*Institute for Astronomy, University of Edinburgh, Royal Observatory, Blackford Hill, Edinburgh EH9 3HJ*
[5]*Laboratoire AIM-Paris-Saclay, CEA/DSM/Irfu – CNRS – Université Paris Diderot, CE-Saclay, pt courrier 131, F-91191 Gif-sur-Yvette, France*
[6]*Astrophysics Group, Imperial College London, Blackett Laboratory, Prince Consort Road, London SW7 2AZ*
[7]*California Institute of Technology, 1200 E. California Blvd., Pasadena, CA 91125, USA*
[8]*Jet Propulsion Laboratory, 4800 Oak Grove Drive, Pasadena, CA 91109, USA*
[9]*Instituto de Astrofísica de Canarias (IAC), E-38200 La Laguna, Tenerife, Spain*
[10]*Departamento de Astrofísica, Universidad de La Laguna (ULL), E-38205 La Laguna, Tenerife, Spain*
[11]*Department of Astrophysical and Planetary Sciences, CASA 389-UCB, University of Colorado, Boulder, CO 80309, USA*
[12]*Observational Cosmology Lab, Code 665, NASA Goddard Space Flight Center, Greenbelt, MD 20771, USA*
[13]*Cardiff School of Physics and Astronomy, Cardiff University, Queens Buildings, The Parade, Cardiff CF24 3AA*
[14]*Dipartimento di Astronomia, Università di Padova, vicolo Osservatorio 3, 35122 Padova, Italy*
[15]*Department of Physics & Astronomy, University of British Columbia, 6224 Agricultural Road, Vancouver, BC V6T 1Z1, Canada*
[16]*ESO, Karl-Schwarzschild-Str. 2, 85748 Garching bei München, Germany*
[17]*UK Astronomy Technology Centre, Royal Observatory, Blackford Hill, Edinburgh EH9 3HJ*
[18]*Institut d'Astrophysique Spatiale (IAS), bâtiment 121, Université Paris-Sud 11 and CNRS (UMR 8617), 91405 Orsay, France*
[19]*National Radio Astronomy Observatory, PO Box O, Socorro NM 87801, USA*
[20]*Infrared Processing and Analysis Center, MS 100-22, California Institute of Technology, JPL, Pasadena, CA 91125, USA*
[21]*School of Physics and Astronomy, The University of Manchester, Alan Turing Building, Oxford Road, Manchester M13 9PL*
[22]*Institute for Astronomy, University of Hawaii, Honolulu, HI 96822, USA*
[23]*Canada–France–Hawaii Telescope, Kamuela, HI 96743, USA*
[24]*Astronomy Centre, Department of Physics & Astronomy, University of Sussex, Brighton BN1 9QH*
[25]*Institut d'Astrophysique de Paris, UMR 7095, CNRS, UPMC Univ. Paris 06, 98 bis boulevard Arago, F-75014 Paris, France*
[26]*Mullard Space Science Laboratory, University College London, Holmbury St Mary, Dorking, Surrey RH5 6NT*
[27]*Space Science & Technology Department, Rutherford Appleton Laboratory, Chilton, Didcot, Oxfordshire OX11 0QX*
[28]*Institute for Space Imaging Science, University of Lethbridge, Lethbridge, Alberta T1K 3M4, Canada*

⋆E-mail: veronique.buat@oamp.fr

[29]*Astrophysics, Oxford University, Keble Road, Oxford OX1 3RH*
[30]*Centre for Astrophysics Research, University of Hertfordshire, College Lane, Hatfield, Hertfordshire AL10 9AB*

Accepted 2010 July 6. Received 2010 July 6; in original form 2010 May 20

ABSTRACT

The reliability of infrared (IR) and ultraviolet (UV) emissions to measure star formation rates (SFRs) in galaxies is investigated for a large sample of galaxies observed with the Spectral and Photometric Imaging Receiver (SPIRE) and the Photodetector Array Camera and Spectrometer (PACS) instruments on *Herschel* as part of the *Herschel* Multi-Tiered Extragalactic Survey (HerMES) project. We build flux-limited 250-μm samples of sources at redshift $z < 1$, cross-matched with the *Spitzer*/MIPS and *GALEX* catalogues. About 60 per cent of the *Herschel* sources are detected in UV. The total IR luminosities, $L_{\rm IR}$, of the sources are estimated using a spectral energy distribution (SED) fitting code that fits to fluxes between 24 and 500 μm. Dust attenuation is discussed on the basis of commonly used diagnostics: the $L_{\rm IR}/L_{\rm UV}$ ratio and the slope, β, of the UV continuum. A mean dust attenuation $A_{\rm UV}$ of $\simeq$3 mag is measured in the samples. $L_{\rm IR}/L_{\rm UV}$ is found to correlate with $L_{\rm IR}$. Galaxies with $L_{\rm IR} > 10^{11}\,{\rm L}_{\odot}$ and $0.5 < z < 1$ exhibit a mean dust attenuation $A_{\rm UV}$ of about 0.7 mag lower than that found for their local counterparts, although with a large dispersion. Our galaxy samples span a large range of β and $L_{\rm IR}/L_{\rm UV}$ values which, for the most part, are distributed between the ranges defined by the relations found locally for starburst and normal star-forming galaxies. As a consequence the recipe commonly applied to local starbursts is found to overestimate the dust attenuation correction in our galaxy sample by a factor of ∼2–3. The SFRs deduced from $L_{\rm IR}$ are found to account for about 90 per cent of the total SFR; this percentage drops to 71 per cent for galaxies with SFR $< 1\,{\rm M}_{\odot}\,{\rm yr}^{-1}$ (or $L_{\rm IR} < 10^{10}\,{\rm L}_{\odot}$). For these faint objects, one needs to combine UV and IR emissions to obtain an accurate measure of the SFR.

Key words: galaxies: evolution – galaxies: stellar content – infrared: galaxies – ultraviolet: galaxies.

1 INTRODUCTION

Far-infrared (far-IR) and ultraviolet (UV) luminosities are commonly used to estimate the current star formation rate (SFR) in galaxies since both emissions are expected to come from young stars. By combining observed IR and UV luminosities one can therefore make an energetic budget and derive an accurate measure of the total SFR in star-forming galaxies (e.g. Iglesias-Páramo et al. 2004; Elbaz et al. 2007). It is often the case that only UV or IR data exist, however, and so the question remains of how reliably one can determine SFRs from UV or IR alone.

SFRs derived from dust emission are based on estimates of the total IR luminosity [$L_{\rm IR} = L(8\text{–}1000\,\mu{\rm m})$]. This measure is accurate in the nearby Universe thanks to the observations of *IRAS* and *Spitzer*, both of which sampled the wavelength range close to the peak emission of the dust. *Spitzer* was also used to observe galaxies up to $z \approx 2$ in the mid-IR; however, extrapolation to the total IR luminosity remains uncertain and relies on relations determined from nearby galaxy populations. By observing in the rest-frame far-IR of galaxies, *Herschel*[1] (Pilbratt et al. 2010) allows us to measure accurately this IR bolometric luminosity over a continuous and wide range of redshift.

The main issue when using UV emission to estimate SFRs is the effect of dust attenuation. The $L_{\rm IR}/L_{\rm UV}$ ratio has been identified as a very powerful estimator of dust attenuation in star-forming galaxies (e.g. Gordon et al. 2000; Buat et al. 2005). Dust attenuation diagnostics based on UV data alone must be used when UV and IR rest-frame data are not simultaneously available. Meurer, Heckman & Calzetti (1999) found a relation between the slope of the rest-frame UV continuum β [defined as $f_{\lambda}({\rm erg\,cm^{-2}\,s^{-1}\,nm^{-1}}) \propto \lambda^{\beta}$ for $\lambda > 120$ nm] and dust attenuation traced by $L_{\rm IR}/L_{\rm UV}$ for local starburst galaxies observed by *International Ultraviolet Explorer* (*IUE*) and *IRAS*. This local starburst relation is also widely used to estimate dust attenuation in UV-selected galaxies at high redshift (Burgarella, Le Floc'h & Takeuchi 2007; Reddy et al. 2008). In the local Universe luminous IR galaxies (LIRGs, with $L_{\rm IR} > 10^{11}\,{\rm L}_{\odot}$) are found to roughly follow the local starburst law (Howell et al. 2010; Takeuchi et al. 2010). Normal star-forming galaxies, less active in star formation than starburst ones, do not follow this relation, and the spectral slope β is found to depend on a number of parameters that are not solely related to dust attenuation (e.g. Kong et al. 2004; Buat et al. 2005; Boissier et al. 2007). Checking the validity of β as a tracer of dust attenuation on large samples of galaxies at different redshifts is therefore a key to both understanding dust attenuation processes in galaxies and to being able to correct accurately for extinction.

[1]*Herschel* is an ESA space observatory with science instruments provided by Principal Investigator consortia. It is open for proposals for observing time from the worldwide astronomical community.

In this Letter we will analyse the IR and UV properties of galaxies over the redshift range, $0 < z < 1$. This is the first time accurate estimates of the total dust emission have been determined over a continuous range of redshift by using several IR measurements including new *Herschel* data and which can be compared to the observed UV emission.

2 DATA

Observations of the Lockman field were made with *Herschel* as part of the *Herschel* Multi-Tiered Extragalactic Survey (HerMES[2]; Oliver et al., in preparation). This field was also observed by *GALEX* (Martin et al. 2005) in *FUV* ($\lambda \simeq 153$ nm) and *NUV* ($\lambda \simeq 231$ nm) as part of the Deep Imaging Survey (DIS). Only sources with $z < 1$ are detected by *GALEX* due to absorption by the Lyman break.

Our first parent sample is based on the shallow observations of the Lockman SWIRE field ($10^{\rm h}45^{\rm m}00^{\rm s}$ $+58^{\rm d}00^{\rm m}00^{\rm s}$, 218×218 arcmin^2) with SPIRE (Griffin et al. 2010). We use the HerMES cross-identified catalogue of Roseboom et al. (2010) which is based on a linear inversion method using the positions of sources detected in the *Spitzer* 24-μm surveys. We select 7435 sources that are detected at 5σ or above at 250 μm, corresponding to a limit of 23 mJy (Roseboom et al. 2010). A redshift has been assigned to 3862 sources. Where available, we use spectroscopic redshifts (taken from the NASA/IPAC Extragalactic Database), otherwise photometric redshifts from the Sloan Digital Sky Survey (SDSS)/Data Release 7 (DR7) (Abazajian et al. 2009) and the SWIRE survey (Rowan-Robinson et al. 2008) are used by order of priority. We identify 3824 galaxies with $z < 1$, of which 30 per cent have spectroscopic redshifts. This sample is then cross-matched with the *GALEX* detections in the *NUV* with a tolerance radius of 2 arcsec (based on *Spitzer*/IRAC coordinates): 2426 galaxies are detected in *NUV* with $z < 1$. The UV slope β can be calculated from the $FUV - NUV$ colour for sources with $z < 0.3$. Of the 1542 objects at $z < 0.3$, 1250 are detected in the *NUV* and 943 have both *FUV* and *NUV* fluxes that are of sufficient accuracy ($\Delta m < 0.1$ mag) to enable reliable estimates of β.

Although ∼40 per cent of the Lockman SWIRE sources selected at 250 μm are not detected in the *NUV*, it is quite difficult to study the non-detections since not less than 21 *GALEX* fields with different depths are needed to cover the HerMES field. Therefore we also consider the *Herschel* deep observations of the Lockman-North field [$10^{\rm h}46^{\rm m}00^{\rm s}$ $+59^{\rm d}01^{\rm m}00^{\rm s}$, 35×35 arcmin^2, 5σ limit at 250 μm corresponding to 8 mJy (Roseboom et al. 2010)]: 70 per cent of this field is covered by only three *GALEX* fields, and a check of each individual source by hand is therefore possible. A second advantage of the Lockman-North field is that it was also observed with PACS (Poglitsch et al. 2010) and data at 110 and 160 μm are available. We again use the cross-matched catalogue of Roseboom et al. (2010) and perform a selection and a *GALEX* cross-match similar to that made for the Lockman SWIRE field. Photometric redshifts were determined by Strazzullo et al. (2010) from visible, near-IR and IRAC data. 246 sources are selected at 250 μm, of which 129 galaxies are detected in the *NUV*. The 58 sources that are considered as non-detections in the *NUV* are assigned a limiting magnitude of $NUV = 24.4$ (Morissey et al. 2005). We consider as UV upper limits, objects with no *GALEX* source within 6 arcsec of the SPIRE position (for distances less than 6 arcsec the full *NUV* point spread function falls into the 250-μm one).

[2] http://www.hermes.sussex.ac.uk

Total IR luminosities, $L_{\rm IR}$, are calculated using the CIGALE code (Noll et al. 2009; http://cigale.oamp.fr) with Dale & Helou (2002) and Siebenmorgen & Krügel (2007) IR templates. A Bayesian analysis is performed to deduce physical parameters from the fitting of spectral energy distributions (SEDs) of galaxies. We restrict the analysis to the thermal IR (≥24-μm data), and defer an analysis of the full UV-to-far-IR SEDs to a later paper. For each source we consider all the available data between 24 and 500 μm: by construction we will always have at least two data points. We keep only objects for which the reduced χ^2 of the fit between the best template and the data set is lower than 10 (98 per cent of the initial samples). Typical errors on estimated $L_{\rm IR}$ are found lower than 0.1 dex. UV luminosities $L_{\rm UV}$ are derived at 153-nm rest-frame (*FUV*) by interpolating *FUV* and *NUV* fluxes, a mean $FUV - NUV$ colour is used when *FUV* data are not available, and are defined as the quantities νL_ν. Both $L_{\rm IR}$ and $L_{\rm UV}$ are expressed in solar units. All magnitudes are given in the AB system. We assume that $\Omega_{\rm m} = 0.3$, $\Omega_\Lambda = 0.7$ and $H_0 = 70\,{\rm km\,s^{-1}\,Mpc^{-1}}$.

3 DUST ATTENUATION AS TRACED BY $L_{\rm IR}/L_{\rm UV}$

The ratio of $L_{\rm IR}/L_{\rm UV}$ is a powerful measure of dust attenuation and is known to correlate with the bolometric luminosity of galaxies in the nearby Universe (e.g. Buat et al. 2007a). *Spitzer* observations extended the analysis out to $z \simeq 0.7$ (Buat et al. 2007b; Xu et al. 2007; Zheng et al. 2007). Here we re-investigate this relation using the Lockman-North sample in the redshift range $0 < z < 1$. We choose this field in order to be able to discuss lower limits for galaxies not detected in UV. Shown in Fig. 1 is a plot of $L_{\rm IR}/L_{\rm UV}$ as a function of $L_{\rm IR}$. The mean dust attenuation is $A({\rm UV}) = 3 \pm 1$ mag for the whole sample (using the calibration of Buat et al. 2005). As expected, there is a general increase of $L_{\rm IR}/L_{\rm UV}$ with $L_{\rm IR}$. We measure the mean $L_{\rm IR}/L_{\rm UV}$ ratio within several bins of $\log(L_{\rm IR})$ (using the Kaplan–Meier estimator to

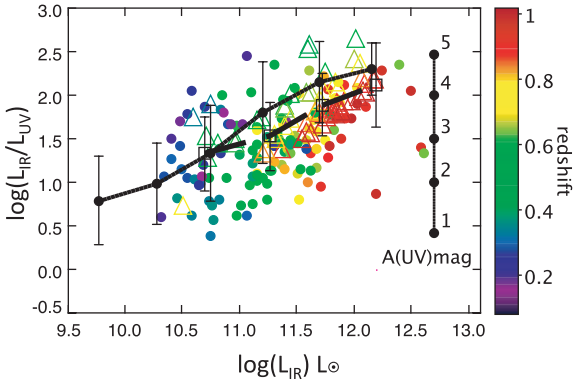

Figure 1. $L_{\rm IR}/L_{\rm UV}$ versus $L_{\rm IR}$ for sources detected in the Lockman-North in the redshift range $0 < z < 1$ (the redshift is colour-coded). Lower limits of $L_{\rm IR}/L_{\rm UV}$ are plotted as triangles for galaxies not detected in UV. The filled circles and solid line correspond to the relation found for local IR-selected galaxies (Buat et al. 2007a), the empty squares and dashed line to the mean values per bin of IR luminosity obtained in this Letter. Error bars correspond to the scatter of the data (1 rms). The A(UV) scale is obtained using the calibration of Buat et al. (2005). The luminosity bins and mean redshift in the bins are $\log(L_{\rm IR}) < 11$ and $\langle z \rangle = 0.4$, $11 \leq \log(L_{\rm IR}) < 11.5$ and $\langle z \rangle = 0.55$, $11.5 \leq \log(L_{\rm IR}) < 12$ and $\langle z \rangle = 0.8$, $\log(L_{\rm IR}) \geq 12$ and $\langle z \rangle = 0.9$.

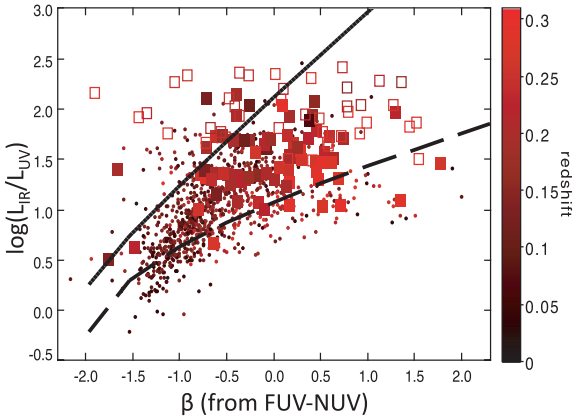

Figure 2. L_{IR}/L_{UV} versus β (the slope of the UV continuum) for galaxies in the Lockman SWIRE field that are also detected in *FUV* and *NUV* ($z < 0.3$): dots represent galaxies with $L_{IR} < 10^{11}$ $L_{\odot}$ and a robust measure of β; filled squares represent LIRGs ($L_{IR} > 10^{11}$ $L_{\odot}$) with a robust measure of β and LIRGs with less reliable β values are represented by empty squares. The redshift of sources is colour-coded. The superposed lines trace the relation found for local starburst galaxies (solid line) and for local normal star-forming galaxies (dashed line).

account for lower limits). The locus of galaxies at low z appears to be consistent with the $z = 0$ relations (Buat et al. 2007a); however, at $z > 0.5$, L_{IR}/L_{UV} is found to be lower by ∼0.3 dex. This difference at higher z is of low statistical significance (of the order of 1σ error bars) and could be affected by the lower limit corrections, but if it is real this implies a decrease in dust attenuation by ∼0.7 mag in the *FUV* for distant, luminous IR-selected galaxies which is consistent with dust attenuation found for LIRGs at $z = 0.7$ by Buat et al. (2007b). A decrease in dust attenuation is possibly linked to a lower metallicity in high-redshift systems. Indeed Reddy et al. (2010) found a correlation between oxygen abundance and dust attenuation in $z \sim 2$ star-forming galaxies. The morphological evolution of LIRGs from mergers to more normal galaxies as z increases can also imply a decrease of dust attenuation (e.g. Buat et al. 2007b, and references therein). Because of a larger gas mass fraction in distant galaxies, the star formation could be spread out over larger, more diffuse and less extinguished regions than in local LIRGs. A decrease of dust attenuation was also reported by Daddi et al. (2007) for ultraluminous IR galaxies between $z = 0$ and ∼2 associated to a longer lived star formation for the higher redshift sources.

4 DUST ATTENUATION AS TRACED BY THE UV SLOPE

A common way to estimate dust attenuation in the UV in the absence of IR data is to use the slope β of the UV continuum. To estimate β from the $FUV - NUV$ colour we focus on galaxies with $z < 0.3$ in the Lockman SWIRE sample and apply the Kong et al. (2004) recipe. A measurement error of 0.1 mag in *FUV* and *NUV* translates into an error of 0.3 for β. Therefore we restrict the analysis (otherwise specified) to sources measured in *FUV* and *NUV* with an accuracy better than 0.1 mag. We have checked that considering the whole sample of galaxies detected in *FUV* and *NUV* does not change the results, only adds a larger dispersion in the diagrams. Shown in Fig. 2 is a plot of L_{IR}/L_{UV} as a function of β, together with local relations for starbursts (Kong et al. 2004) and optically selected star-forming galaxies (Boissier et al. 2007) are superposed. Galaxies from our IR-selected sample exhibit a wide range of β and L_{IR}/L_{UV} values as already found in the nearby Universe (Buat et al. 2005; Seibert et al. 2005; Takeuchi et al. 2010). The majority of the galaxies lie between the two relations, i.e. have a dust attenuation (as defined by L_{IR}/L_{UV}) for a given β that is larger than that found in local normal star-forming galaxies but lower than in local starbursts. From the 164 LIRGs of our initial sample of 1542 sources at $z < 0.3$ in the Lockman SWIRE field, 125 are detected in *NUV* and *FUV*, of which 78 have a reliable estimate of β ($\Delta m < 0.1$ mag in *FUV* and *NUV*) and are shown in Fig. 2. Out of these 78 LIRGs, 67 (i.e. 87 per cent) are found to lie below the local starburst relation. The fraction drops to 77 per cent for the 125 LIRGs detected in both *FUV* and *NUV* without any restriction on the measurement accuracy. 11 per cent of the galaxies (including 10 LIRGs) detected in *NUV* have no *FUV* detection (for these we adopt a limiting *FUV* magnitude of 24.8; Morissey et al. 2005); if we consider only sources with *NUV* magnitudes with $\Delta NUV < 0.1$, all these sources are found below the starburst law. This estimate might be uncertain given the large number of *GALEX* fields with different exposure times. As quoted in Section 2, 23 per cent of the initial sample at $z < 0.3$ are detected neither in *NUV* nor in *FUV*: the limiting magnitude of $NUV = 24.4$ roughly corresponds to a limit on L_{IR}/L_{UV} of ≃200 in the redshift range $0 < z < 0.3$ (for the lowest IR luminosities at each redshift). Therefore we miss at most 23 per cent of galaxies with $\log(L_{IR}/L_{UV}) > 2.3$ (note that fewer than 23 per cent may be genuine non-detections as discussed for the Lockman-North field). A detailed discussion of UV non-detections is deferred to a future paper. Nevertheless, even if we account for galaxies not detected in the *NUV* and *FUV*, a substantial fraction of all the IR-selected galaxies is found below the local starburst law. Dust attenuation in these galaxies is *overestimated* if the recipe for starburst galaxies based on the UV spectral slope is applied.

The most distant galaxies of our sample, including LIRGs, are found to depart strongly from the starburst law (see Fig. 2). β is calculated from the observed $FUV - NUV$ colour: the wavelengths sampled go from 150 and 230 nm at $z = 0$ to 118 and 180 nm at $z = 0.3$. Therefore, the power-law model for the UV continuum assumed to calculate β might not be valid for the whole 118–230 nm range and for dust attenuations ranging from 0.5 to 5 mag in UV. The uncertainty can also be amplified because of the rather large bandwidths of the *GALEX* filters (Morissey et al. 2005). Variations in dust properties and star versus dust geometry are known to induce large dispersions in the L_{IR}/L_{UV}–β diagram (Gordon et al. 2000; Boquien et al. 2009). Our selection at 250 μm may also lead to more quiescent galaxies than local LIRGs in terms of star formation which is known to increase β for a given L_{IR}/L_{UV} (Kong et al. 2004). At $z = 2$, Reddy et al. (2010) found that Lyman break galaxies also detected at 24 μm and with bolometric luminosity lower than 10^{12} $L_{\odot}$ follow the local starburst law, although with a large dispersion. These galaxies have $\beta < -0.5$ and therefore are much bluer than the bulk of our sample. At high redshift the dynamical range in stellar population is narrower and the contribution to the UV continuum of stars not related to the current star formation is likely to be negligible in star-forming galaxies at $z > 1$. The spatial distribution of dust and young stars may also be similar to that found in strong local starbursts making the law proposed by Meurer et al. (1999) more appropriate for these high-redshift objects than for our present sample.

This topic will be re-investigated in a future work by fitting the whole SED from the UV to the IR both at low and high redshifts.

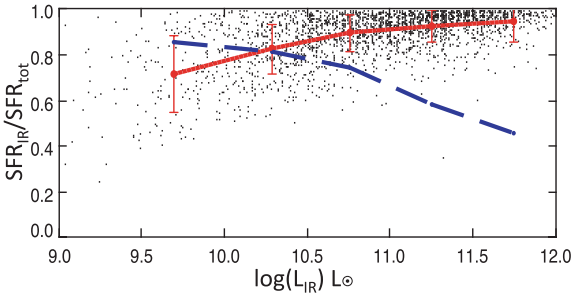

Figure 3. Fraction of SFR measured in IR, SFR_{IR} as a function of the IR luminosity, L_{IR}. The mean and standard deviation of the values in five bins of $\log(L_{IR})$: <10, 10–10.5, 10.5–11, 11–11.5, >11.5 are shown in red, joined by a solid line to guide the eye. The blue dashed line represents the fraction of galaxies detected in the UV at each value of $\log(L_{IR})$.

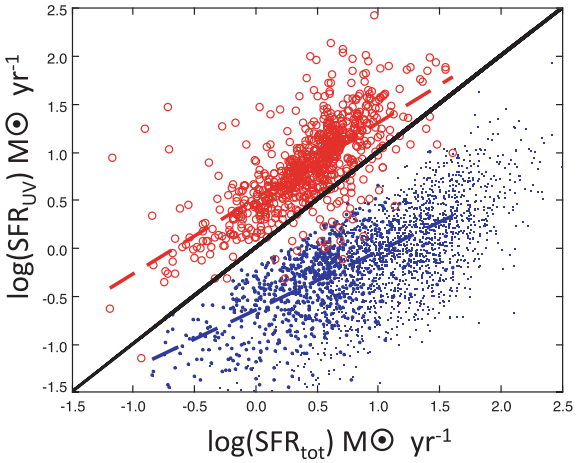

Figure 4. A plot of SFR_{UV} versus SFR_{tot}, where $SFR_{tot} = SFR_{IR} + SFR_{UV}$. SFRs deduced from uncorrected UV fluxes are plotted with blue dots, the largest ones correspond to galaxies at $z < 0.2$. SFRs deduced from UV fluxes corrected for dust attenuation with the relation of Meurer et al. (1999) are plotted with open red circles for galaxies with $z < 0.2$. The linear regression lines between SFR_{tot} and the two estimates of SFR_{UV} are plotted as dashed lines. The black solid line corresponds to equal values on both axes.

5 CALIBRATING MEASURES OF STAR FORMATION RATE

An important check is to test whether IR emission alone provides a robust estimate of the total SFR over the whole range of IR luminosities or if ignoring the direct UV light leads to systematic errors. We again use the sample derived from the Lockman SWIRE field because of the large number of galaxies in the sample.

We take $SFR_{IR} + SFR_{UV} = SFR_{tot}$ as a reference for the SFR measure where $\log(SFR_{IR})_{M_\odot\,yr^{-1}} = \log(L_{IR})_{L_\odot} - 9.97$ and $\log(SFR_{UV})_{M_\odot\,yr^{-1}} = \log(L_{UV})_{L_\odot} - 9.69$. The UV emission is not corrected for dust attenuation and we use the SFR calibrations from Buat et al. (2008) with the assumption of a constant SFR over 10^8 yr and a Kroupa initial mass function (Kroupa 2001).

Plotted in Fig. 3 is the SFR fraction measured by the IR luminosity, SFR_{IR}/SFR_{tot}, as a function of L_{IR}, with an additional curve showing the fraction of the galaxies in the sample with that IR luminosity that are detected in the UV. When the sample is considered as a whole, we find that SFR_{IR} measures ∼90 per cent of the total SFR. This fraction varies with L_{IR}: from 94 ± 10 per cent for the most luminous galaxies of our sample ($L_{IR} > 10^{11.5}\,L_\odot$) with 45 per cent detected in UV, down to 71 ± 17 per cent when $L_{IR} < 10^{10}\,L_\odot$ or equivalently $SFR_{tot} < 1\,M_\odot\,yr^{-1}$ and a UV detection rate reaching 85 per cent. This demonstrates that the combination of obscured and unobscured SFRs is required to determine accurate SFRs in galaxies with low star formation activity. Intrinsically faint galaxies detected in rest-frame UV surveys are found to be a significant component of luminosity functions and of the total star formation density at both low and high redshifts (Buat et al. 2007a; Reddy & Steidel 2009). As a consequence, both UV- and IR-selected samples must be built and their contribution added to measure the total star formation density at a given redshift (Iglesias-Páramo et al. 2006; Reddy & Steidel 2009).

Shown in Fig. 4 is a comparison of the SFR measured in the UV with SFR_{tot}, for both uncorrected and corrected UV luminosities, where the correction used is that of Meurer et al. (1999): $A_{UV} = 4.43 + 1.99\beta$ deduced from their L_{IR}/L_{UV}–β relation. For this correction we only consider galaxies with $z < 0.2$ to narrow the wavelength range used to calculate β. Without dust attenuation corrections, SFR_{UV} underestimates the total SFR by a factor of ∼6 for $SFR_{tot} \simeq 1\,M_\odot\,yr^{-1}$ and ∼30 for $SFR_{tot} \simeq 100\,M_\odot\,yr^{-1}$. As expected from Fig. 2, with dust corrections based on β, SFRs are overestimated by a factor of ∼2–3. At $z \sim 1$, Elbaz et al. (2007) only obtain $SFR \leq 10\,M_\odot\,yr^{-1}$ when correcting UV luminosities for dust attenuation based on values of β. They use the $U - B$ colour to measure β which corresponds to the wavelength range 180–225 nm at $z \sim 1$, which is different from the ranges used in this Letter and by Meurer et al. (1999). Burgarella et al. (2007) and Reddy & Steidel (2009) corrected UV measurements using the L_{IR}/L_{UV}–β relation for local starbursts and found SFR deduced from UV-corrected luminosities to be in agreement with SFR_{tot} out to few hundreds $M_\odot\,yr^{-1}$, albeit with significant dispersion. As discussed in Section 4, this agreement is likely to be due to the different nature of UV-selected galaxies at $z > 1$ as compared to the IR-selected galaxies analysed in this Letter.

ACKNOWLEDGMENTS

SPIRE has been developed by a consortium of institutes led by Cardiff University (UK) and including University of Lethbridge (Canada); NAOC (China); CEA, OAMP (France); IFSI, University of Padua (Italy); IAC (Spain); Stockholm Observatory (Sweden); Imperial College London, RAL, UCL-MSSL, UKATC, University of Sussex (UK) and Caltech/JPL, IPAC, University of Colorado (USA). This development has been supported by national funding agencies CSA (Canada); NAOC (China); CEA, CNES, CNRS (France); ASI (Italy); MCINN (Spain); SNSB (Sweden); STFC (UK) and NASA (USA). The data presented in this Letter will be released through the *Herschel* Database in Marseille HeDaM (http://hedam.oamp.fr/HerMES). This Letter makes use of TOPCAT, http://www.star.bristol.ac.uk/mbt/topcat/.

REFERENCES

Abazajian K. N. et al., 2009, ApJS, 182, 543
Boissier S. et al., 2007, ApJS, 173, 524
Boquien M. et al., 2009, ApJ, 706, 553
Buat V. et al., 2005, ApJ, 619, L51
Buat V. et al., 2007a, ApJS, 173, 404
Buat V., Marcillac D., Burgarella D., Le Floc'h E., Takeuchi T. T., Iglesias-Páramo J., Xu C. K., 2007b, A&A, 469, 19
Buat V. et al., 2008, A&A, 483, 107
Burgarella D., Le Floc'h E., Takeuchi T. T., Huang J. S., Buat V., Rieke G. H., Tyler K. D., 2007, MNRAS, 380, 986

Daddi E. et al., 2007, ApJ, 670, 156
Dale D. A., Helou G., 2002, ApJ, 576, 159
Elbaz D. et al., 2007, A&A, 468, 33
Gordon K. D., Clayton G. C., Witt A. N., Misselt K. A., 2000, ApJ, 533, 236
Griffin M. et al., 2010, A&A, 518, L3
Howell J. H. et al., 2010, ApJ, 715, 572
Iglesias-Páramo J., Buat V., Donas J., Boselli A., Milliard B., 2004, A&A, 419, 109
Iglesias-Páramo J. et al., 2006, ApJS, 164, 38
Kong X., Charlot S., Brinchmann J., Fall S. M., 2004, MNRAS, 349, 769
Kroupa P., 2001, MNRAS, 322, 231
Martin D. C. et al., 2005, ApJ, 619, L1
Meurer G. R., Heckman T. M., Calzetti D., 1999, ApJ, 521, 64
Morissey P. et al., 2005, ApJ, 619, L7
Noll S., Burgarella D., Giovannoli E., Buat V., Marcillac D., Muñoz-Mateos J. C., 2009, A&A, 507, 1793
Pilbratt et al., 2010, A&A, 518, L1
Poglitsch A. et al., 2010, A&A, 518, L2
Reddy N. A., Steidel C. C., 2009, ApJ, 692, 778
Reddy N. A., Steidel C. C., Pettini M., Adelberger K. L., Shapley A. E., Erb D. K., Dickinson M., 2008, ApJS, 175, 48
Reddy N. A., Erb D. K., Pettini M., Steidel C. C., Shapley A. E., 2010, ApJ, 712, 1070
Roseboom I. et al., 2010, MNRAS, submitted
Rowan-Robinson M. et al., 2008, MNRAS, 386, 697
Seibert M. et al., 2005, ApJ, 619, L55
Siebenmorgen R., Krügel E., 2007, A&A, 461, 445
Strazzullo V., Pannella M., Owen F. N., Bender R., Morrison G. E., Wang W.-H., Shupe D. L., 2010, ApJ, 714, 1305
Takeuchi T. T., Buat V., Heinis S., Giovannoli E., Yuan F.-T., Iglesias-Páramo J., Murata K. L., Burgarella D., 2010, A&A, 514, A4
Xu C. K. et al., 2007, ApJS 173, 432
Zheng X. Z., Dole H., Bell E. F., Le Floc'h E., Rieke G. H., Rix H.-W., Schiminovich D., 2007, ApJ, 670, 301

This paper has been typeset from a TEX/LATEX file prepared by the author.